IEEE Photonics Journal
An IEEE Photonics Society Publication

Open Access

Integrating Backlight With Color-Filter-Free Panel for Enhancing Performance of LCD

Volume 12, Number 1, February 2020

Tun-Chien Teng
Chun-Hao Sun

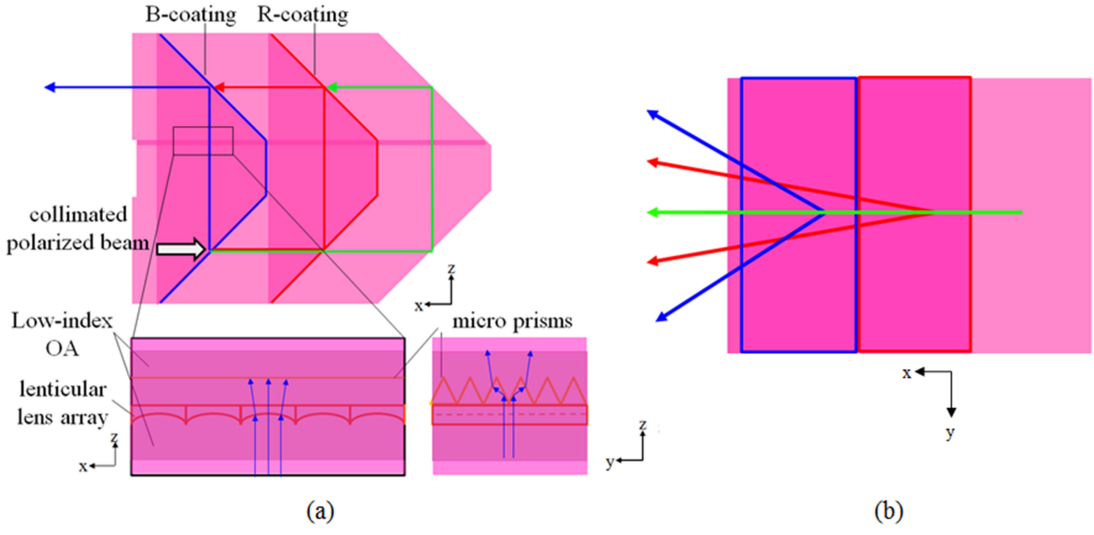

DOI: 10.1109/JPHOT.2019.2957385

Integrating Backlight With Color-Filter-Free Panel for Enhancing Performance of LCD

Tun-Chien Teng and Chun-Hao Sun

Department of Mechatronic Engineering, National Taiwan Normal University, Taipei 106, Taiwan

DOI:10.1109/JPHOT.2019.2957385

Manuscript received September 25, 2019; revised November 21, 2019; accepted November 30, 2019. Date of publication December 3, 2019; date of current version January 7, 2020. This work was supported by the Ministry of Science and Technology of Taiwan under Grant MOST 105-2221-E-003-009 and MOST 107-2221-E-003-015 MY3. Corresponding author: Tun-Chien Teng (e-mail: walter.teng@ntnu.edu.tw).

Abstract: In this study, we proposed an innovative concept of integrating a polarized color-separating backlight with a color-filter-free LC panel for enhancing performance of the curved LCD system. We design a two-level folded backlight to exploit the light sources LEDs with color enhancement by quantum-dot technology to produce color beams emerging at separate angles with a linearly polarizing state. The integrated LC panel focuses the separating color beams onto the corresponding subpixels with no need of the color filter; redirects the color beams at respective angles into the normal and reforms their angular shapes to be identical for attaining good color uniformity in the viewing cone. We established a system model for simulation to evaluate its performance. According to the simulation results, it performs the high optical efficiency of 33.75% that is about four times the traditional LCD, and displays color gamut of 94.1% NTSC (CIE 1931). It also provides the illuminance uniformity of 90% above and good color uniformity in both the spatial space and angular space of the viewing cone with horizontal and vertical angular widths of 100° and 75°, respectively. Furthermore, the simulation results demonstrate that the design can apply to a 55-inch curved LCD and further extend the maximum diagonal size up to 88 inches while keeping slim volume with a minimal thickness of 6.5 mm.

Index Terms: Displays, illumination design, light-emitting diodes, nonimaging optics, polarization-selective devices, microstructure fabrication.

1. Introduction

The rapid development of liquid crystal (LC) panel technology has caused the liquid crystal display (LCD) become widely used in various devices, ranging from large products to small products. Recently, the market for organic light-emitting diode (OLED) displays has grown rapidly and has started to challenge LCDs in all applications, especially in the small-sized display market. However, each technology has its own pros and cons, so the competition between them is still ongoing and they will coexist for a long time [1]. Therefore, researches on LCD for providing optimal display quality, greater functionality, and the energy-conservation properties are still important. Although technological advancements have improved the energy efficiency of LCD technologies, the overall optical efficiency remains relatively low. In general, less than 10% of the light from an LCD backlight module passes through the LC panel, primarily because of the polarizer and color filter in the LC panel. The polarizer absorbs at least 50% of the incident light and transmits the remainder

as linearly polarized light; the color filter further absorbs at least two thirds of the polarized light propagating through the polarizer; consequently, the light from a backlight module transmitting the LC panel is 16% at most in theory. Therefore, developing a polarized backlight first became an attractive research topic.

The design concepts of polarized backlight include as follows. The first concept involves using a multilayer stack of thin film composed of birefringence materials to linearly polarize the light from the backlight (e.g., the most common used is so-called "dual brightness enhancement film (DBEF)" proposed by 3M Ltd. Corp.) [2], [3]. In a similar way, stacking a layer composed of birefringent material on microstructures of the light guide plate (LGP) surface to make them selectively reflect the light linearly polarizing in one direction out of the LGP (p-wave or s-wave only) [4]–[7]. The second concept involves forming a subwavelength grating with double-layer materials on the surface of an LGP or on a film substrate to induce the light to emerge in a linearly polarized state [8]–[13]. However, fabricating subwavelength gratings on a large area of a substrate or LGP surface is extremely difficult. Moreover, the performance is critically dependent on both the wavelength and angle of the incident light. The third concept involves using a specific type of LGP that preserves the polarization state of the polarized light source (polarized LED or LD) to provide the linearly polarized emerging light [14], [15]. However, because the light propagating in the LGP requires sufficiently mixing to form a uniform planar light source, the degree of polarization inevitably reduces during the mixing process. To mitigate this issue, people proposed an approach to make the light from the light source mix uniformly, then polarize, and finally enter the LGP with the polarization state preserved [16].

In addition to the research on the polarized backlight, reducing the absorption in the color filter is another attractive research topic. Eliminating or reducing the absorption in the color filter has two ways: adopting a color-filter-free device or a selectively reflecting filter. Color-filter-free devices include the field sequential color display (FSCD) and color separation display. The FSCD does not require a color filter and subpixels; thereby increase the entire transmittance considerably. However, the FSCD has problems of color breakup and the fast scan rate [17]. In the color separation display, the light emerging from a backlight separates into three primaries of red, green, and blue to pass through the corresponding subpixels, considerably increasing the entire transmittance. According to the working principle of the color separation display, the proposed approaches include two types, diffractive optics and geometrical optics. The approaches involved with diffractive optics are as follows. The first is introducing a sandwich-grating structure to deflect the three primaries into different diffractive orders to separate them spatially [18]. Another similar way is integrating dual gratings and dual lenticular lenses into a hybrid structure to distribute the incident light spatially and laterally according to its wavelengths [19]. The second is combining a blazed grating and a microlens array. The grating angularly distributes the incident light according to its wavelengths, and the microlens array focuses these angularly distributed light beams at their corresponding positions in the focal plane [20]–[25]. However, a grating with the small pitch is required to facilitate angular separation of the three primaries, but the small pitch reduces the optical transmission efficiency; therefore, this contradiction reduce the feasibility of these approaches. Moreover, they are not suitable for the broadband light source because the grating is very sensitive to wavelengths of the incident light. The approaches involved with geometrical optics use the geometric optical element such as a huge lenticular lens, a wedge-shaped light-guide plate (LGP) with a spherical thick end, or three independent collimating elements, to produce the required angularly separated collimated primaries that then focus onto the corresponding subpixels through a lenticular lens array [26]–[28]. Another approach applied in a direct-lit backlight is using a lenticular lens array with grouped lens elements to focus the linear light sources of the three primaries onto the corresponding subpixels directly [29]. As compared with the diffractive-optics approach, the geometrical-optics approach has no contradiction between angular separation and optical efficiency. Moreover, the geometrical optical element has much less sensitive to wavelengths than the diffractive. However, it has a fatal disadvantage that the primaries emerging out of the LC panel at their respective angles leads to color unevenness for the observer in the angular space. Therefore, it would be a feasible solution only if this issue is resolved.

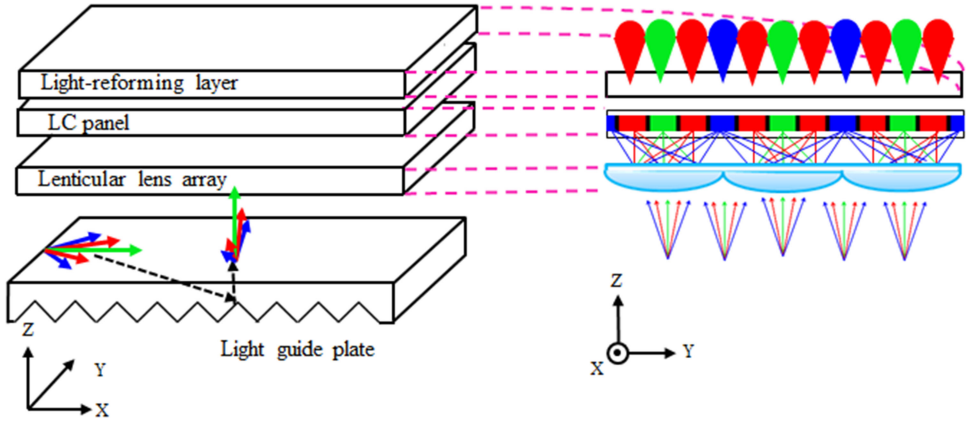

Fig. 1. Scheme of a LC panel operating with a color-separation backlight.

In the selectively reflecting color filter, there are three kinds of subwavelength gratings corresponding to R, G, and B subpixels in the color filter [30]–[34]. An ideal subwavelength grating with a specific pitch transmits one primary and completely reflects the other two primaries. However, the practical subwavelength grating cannot completely reflect the other two primaries so an absorptive color filter is still necessary. Moreover, it is difficult for fabricating the subwavelength grating of multilayers in a large area.

In theory, the polarized backlight can double the optical efficiency, and the color-filter-free device can further triple the optical efficiency; therefore, a well-designed device combining the two functions can greatly improve the optical efficiency of the LCD. The selectively reflecting color filter using subwavelength of two-layer materials does not only filter the primaries but also functions as a polarizer (e.g., transmitting the TM wave but reflecting the TE wave, and vice versa). However, because it cannot convert the polarization state of the reflected light TE wave, it needs a recycling mechanism to convert the TE wave into the TM wave for completely exploiting the light; Yet, the recycling mechanism inevitably causes light-scattering and extra absorption (For DBEF, the practical gain value is about $1.2 \sim 1.77$, below the theoretical value 2 [35], [36]). Moreover, the color filter absorbs part of the light. Therefore, we designed an apparatus of integrating a polarized color-separating backlight with a color-filter-free LC panel for completely exploiting the light from the LEDs with color enhancement by quantum-dot technology and displaying high color gamut. In addition, the apparatus has a curved slim profile and can extend to a large-sized area for applying to the new-fashioned large curved LCD.

2. Design Concept and Model Principle

The system consists of a polarized color-separating backlight and a color-filter-free LC panel. We proposed a backlight for converting the light into the polarized light and separating it into highly collimated R, G, and B color beams for the LC panel. The LC panel has a lenticular lens array thereunder and a light-reforming layer thereon. The lenticular lens array focuses the color beams onto the corresponding subpixels with no need of the color filter; the light-reforming layer redistributes angular shapes of the focused color beams into the same and induces their peaks in the normal direction. The working concept of the system refers to Fig. 1. To accommodate the components and attain a narrow bezel (frame), we adopt a backlight of a two-level folded structure. The light sources LEDs, light mixing-and-collimating elements, polarization-converting elements, and color-separating elements are in the lower level; a monolithic curved LGP is in the upper level. To reduce the entire thickness of the backlight, we adopt the white LED with color enhancement by quantum-dot technology. The following paragraphs detail the functions and mechanism of the related components.

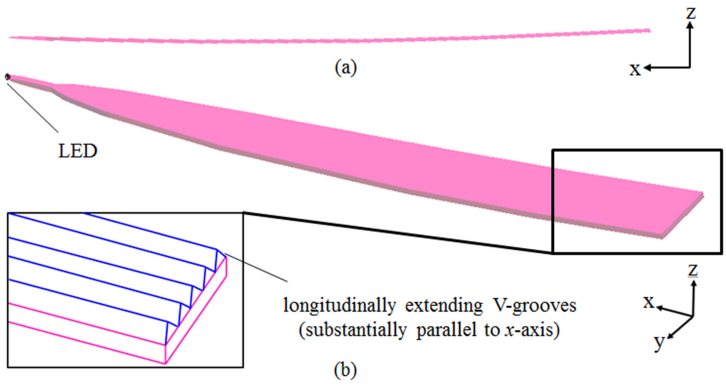

Fig. 2. Scheme of light mixing-and-collimating element.

2.1 Light Mixing-and-Collimating Element

The function of this element is to transfer the light from a Lambertian light source LED into a uniform collimated light source of a rectangular shape (called 'linear beam'), which is necessary for the next two elements to function well. The element is generally composed of two 2D-CPCs (Compound Parabolic Collector) as shown in Fig. 2: one has a varying thickness to converge the vertical angular distribution of the light propagating within it; the other has a varying width to converge the transverse angular distribution. Hereafter, the 'thickness' and 'vertical' are about in the *z*-direction; the 'width' and 'transverse' are about in the *y*-direction; the 'longitudinal' is about along the *x*-axis. CPC converts the divergent light entering its inlet of a small area into a collimated light beam emerging from its outlet of a large area. The relationship between the half-angles of the light entering the inlet and emerging form the outlet are as follows:

$$\frac{t_1}{t_2} = \frac{n_2 \sin \theta_2}{n_1 \sin \theta_1}, \tag{1}$$

where t_1 and t_2 is the thickness (or width) of the inlet and outlet of the CPC, respectively; n_1 and n_2 is the refractive index of the ambient material of the inlet and outlet, respectively. It means that the emerging light with a smaller half-angle needs the element with larger volume. To make the inside propagating light sufficiently mix to become uniform and axially symmetric distribution, the top surface of the element has longitudinally extending micro V-grooves thereon. Then, array the elements side by side to extend in the transverse direction to form a collimated, wide, linear beam emerging from the outlets. The detail can refer to our prior study [16]. To match the curved LC panel, the element has the same curvature radius as the curved LC panel in the longitudinal direction (i.e., *x*-direction). According to the prior study, an incident beam with a small half-angle benefits the converting efficiency of the polarization-converting element, but the half-angle depends on the dimensions of the light mixing-and-collimating element. In addition, the different color beams emerging from the LGP must avoid overlapping each other for color separation. If the half-angle is not small enough, the angle between two color beams must increase, leading to color unevenness in the angular space. With considering the trade-off between the angle and the half-angle, we set the angle between two color beams at 17° and the half-angle of the color beam below 8.5°.

2.2 Polarization-Converting Element

The function of this element is to convert the collimated unpolarized light from the preceding element into polarized light. We transform the reflective-type element in our prior work [16] into a one-pass transmissive type, which has a series of sloped facets to reflect incident light and rotate its polarization direction. Figs. 3(a) & (b) show polarization-converting mechanism as follows. The

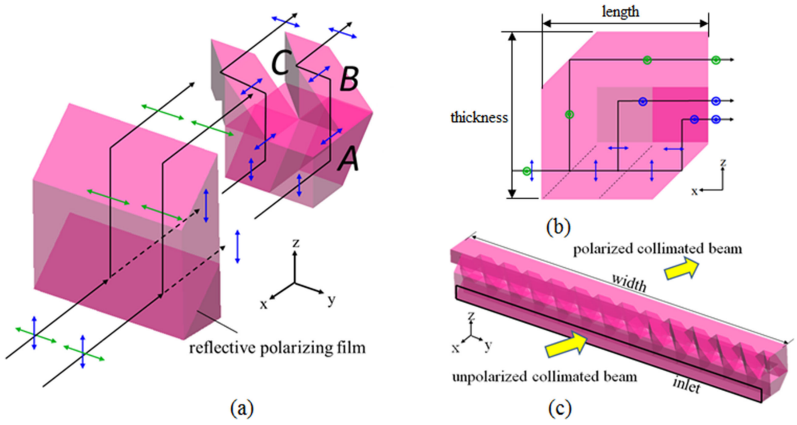

Fig. 3. Polarization-converting element: (a) mechanism of polarization conversion in one unit; (b) side view of (a); (c) plural units assembling a polarization-converting element.

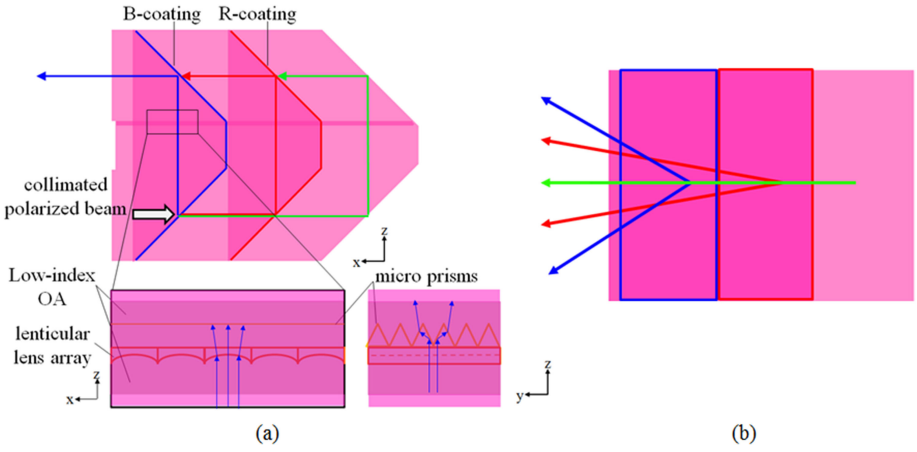

Fig. 4. Color-separating element: (a) side-view, the below two insets are the views of local details of the angle-modulating component; (b) top-view.

unpolarized collimated beam entering the element hits the polarization beam-splitting facet with a reflective polarizing film thereon; and splits into the two polarized collimated beams, a reflective s-wave and a transmission p-wave. The s-wave goes upward and hits a 45°-sloped facet to deflect into the negative x-direction; the p-wave continuously hits the sequential three 45°-sloped facets (A, B, and C) to rotate its polarization direction into a s-wave exiting toward the negative x-direction. Finally, the unpolarized collimated beam is converted into the s-wave. All the slope facets in the element are uncoated except the polarization beam-splitting facet. We exploit the total internal reflection (TIR) of the highly collimated incident light on the sloped facets to reduce the absorption loss greatly. In addition, we array multiples of the unit in Fig. 3(a) side by side to extending in the transverse direction to convert an unpolarized linear beam from the previous element into a polarized linear beam, as shown in Fig. 3(c).

2.3 Color-Separating Element

To split the polarized light from the preceding element into five angularly separated color beams in the transverse direction, the color-separating element comprises six 45°-sloped coating facets and an angle-modulating component, as shown in Fig. 4(a). Three coating facets are in the upper

level and the other three are in the lower level: the left two coating facets with dichroic coating layer are marked as 'B-coating', the middle two coating facets with dichroic coating layer are marked as 'R-coating', and the right two facets are specular mirrors. The B-coating reflects the blue light (called 'B') and passes the other portion of the light; the R-coating reflects the red light (called 'R') and passes the other portion of the light; the right specular mirrors reflect the remaining green light (called 'G'). The angle-modulating component is located in the middle layer between the upper and lower levels. The component is generally a substrate and sandwiched between two layers of optical adhesion of low refractive index (low-index OA), which has micro prisms longitudinally extending in the *x*-axis thereon and an array of micro lenticular lenses transversely extending in the *y*-axis thereunder (refer to the below insets in Fig. 4(a)). The prism has a profile of an isosceles triangle for inducing the incident light along the z-axis to deflect at angles of $\pm\alpha$ with the *z*-axis in the *yz*-plane, and the deflected angle depends on the apex angle of the prism. We control deflected angles of R, G, and B beams separately by modulating apex angles of the corresponding prisms. The lenticular lens array is for diffusing the incident light a little in the *xz*-plane to adjust the tendency of the light emerging out of the LGP and the sequential illuminance distribution on the top surface of the LGP. The lens with a smaller curvature radius diffuses the incident light more so the light tends to emerge out in the front part of the LGP. Therefore, we can modulate the curvature radii of the corresponding lenticular lenses separately to makes the illuminance distribution of the R, G, and B beams smooth and identical, which is very important for the light emerging from the LGP to perform good spatial uniformity in both illuminance and color.

The traveling paths of the incident light are as follows (Refer to Fig. 4). First, the light reflects upward by the coating facets in the lower level and separates into three beams R, G, and B. Second, the beams enter the angle-modulating component. The lenticular lens array diffuses the beams R, G, B in the *xz*-plane; then the prisms split the beams B, R into four beams (2 for R, 2 for B) at their respective deflected angles with z-axis in the *yz*-plane. The two split beams B are symmetrical with z-axis, and so do the two split beams R. The beam G does not split and deflect because the portion corresponding to the beam G has no V-grooves. Third, the five beams (B, R, G, R, and B) further reflect by the coating facets and specular mirror in the upper level and become the light propagating at angles of $\pm\alpha$ with the *x*-axis in the *xy*-plane, as shown in Fig. 4(b). Finally, the incident collimated polarized light is transformed into five collimated polarized color beams (B, R, G, R, B) propagating with their respective angles with the x-axis in the *xy*-plane. Such arrangement of the five color beams is beneficial to reduce the thickness of the LGP and suitable for the curved LGP.

2.4 Curved LGP With Micro V-Grooves

The five collimated polarized color beams from the color-separating element enter the curved LGP. To match a curved LC panel, the LGP in the upper level is designed as a curved with the same curvature radius as the LC panel. Moreover, to preserve the polarization state of the light and keep the difference in the transverse angular space between the five color beams, the LGP has smooth micro V-grooves transversely extending on its bottom surface to reflect the incident light directly upward to emerge out of its top surface. The cross-sectional profile of the V-groove is isosceles. The five collimated polarized color beams emerging from the LGP substantially propagate in the *yz*-plane and keep their respective angles with the z-axis to avoid overlapping one another in the angular space. The V-groove on the LGP bottom can be designed as one with the bare surface or with reflective coating layer. In our design, the light entering the LGP has to be highly collimated previously with an angular range about 10 degrees, and thus most of the light hitting the V-grooves can be reflected by TIR. The detail will be discussed in the next section.

2.5 Integrated Color-Filter-Free LC Panel

We designed an integrated color-filter-free LC panel for cooperating with the five separated collimated color beams emerging from the LGP at different angles with the z-axis, as shown in Fig. 5. The LC panel has a lenticular lens array on its bottom and a light-reforming layer on its top. The

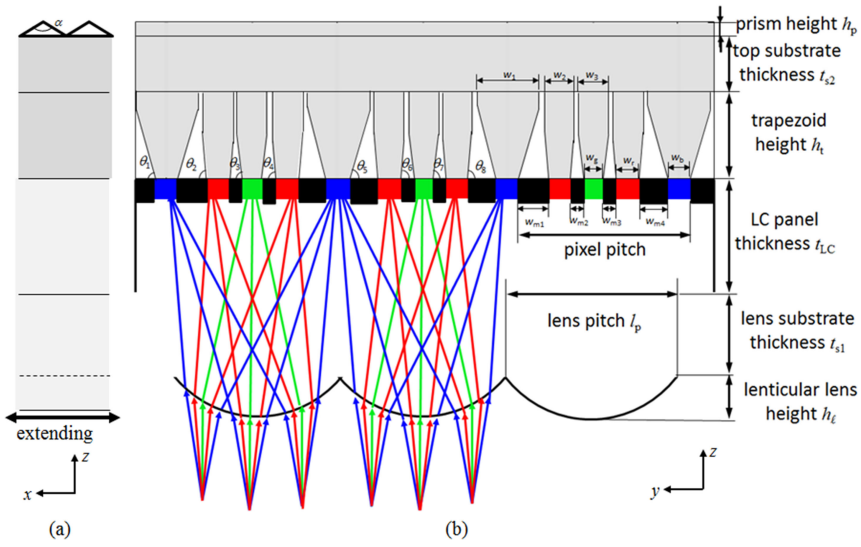

Fig. 5. Scheme of the integrated color-filter-free LC panel: (a) side view; (b) front view.

array of lenticular lenses with a free-form cross-sectional profile extends in the x-direction; its focal plane substantially coincides with the pixel plane. Each lenticular lens has a pitch of one pixel comprising four subpixels with a black matrix intervening and aligns with a pixel of the LC panel, so the five color beams focus onto their corresponding subpixels through the lenses with no need of color filters. However, there is a serious disadvantage in such color separation because the color five beams emerging from the LC panel at their respective angles leads to color unevenness in the viewing cone. To address the issue, we designed a light-reforming layer to modulate the respective angular distribution of the five color beams to be identical and to make the beams emerge out in the normal. The layer consists of a substrate and arrayed microstructures. The substrate (called 'top substrate') has arrayed prisms on the top and microstructures of substantially inverted trapezoids in cross-sectional profile on the bottom. The arrayed inverted trapezoids extend in the x-direction and have three types of sloped side facets corresponding to the slanted incident beams through the LC panel, which redirect incident beams into the normal and reform their angular distribution to be identical in the *yz*-plane. The arrayed prisms extend in the y-direction and further spread their angular distribution in the *xz*-plane. Moreover, there are some silica beads added in the top substrate for further spreading and smoothing the angular distribution of the resultant emerging light to improve its color uniformity in the angular space.

3. Simulation Results and Discussion

In order to evaluate the performance of the proposed LCD system, we established two optical models a polarized color-separating backlight and an integrated color-filter-free LC panel for a series of simulations. The parameters used in the backlight model are as follows. Two pieces of 13.5-lumen LEDs (NS2W364F-HG, Nichia Corp, Japan) with emitting area of 3.3 mm $\times$ 0.3 mm are the white light sources whose luminous intensity is of approximately Lambertian distribution. To reduce the simulation time, the optical model of the backlight comprises only two LEDs, two light mixing-and-collimating elements arranged side by side, a polarization-converting element, a color-separating element, and a curved LGP with an area of 1100 mm $\times$ 80 mm (respectively in x and y directions), as shown in Fig. 6. Both side boundaries of the model were assumed to have completely specular reflective properties, and therefore the simulation results of the model in Figs. 6 (a), (b) were fully equivalent to those of combining the plural identical models to extend transversely in the y direction as shown in Fig. 6(c). Moreover, the model takes both Fresnel loss

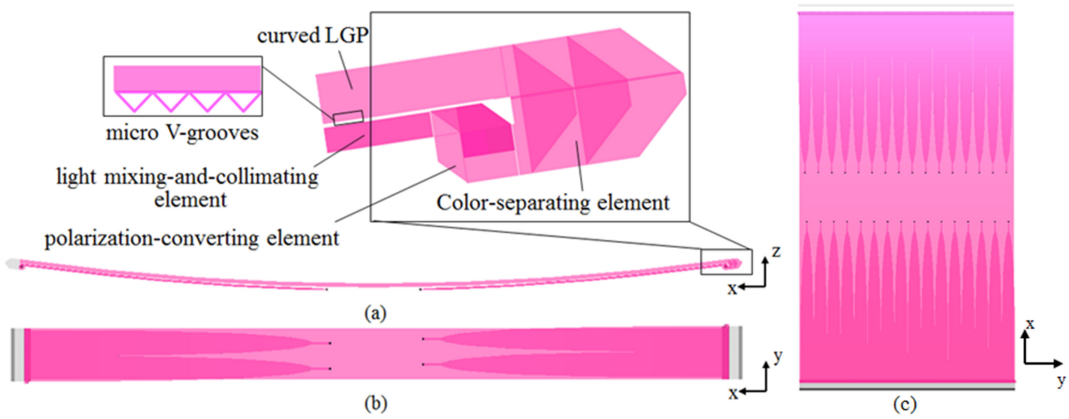

Fig. 6. Scheme of the proposed backlight: (a) side view and local detail drawing inset; (b) bottom view; (c) model in (b) extending transversely in the y direction.

and material absorption into account. The simulation tool used in this study is commercial software 'LightTools' launched by Synopsys Inc. [37].

Similarly, to reduce the simulation time for the integrated LC panel model (Refer to Fig. 5), the width (in the y-direction) of the optical model is only one pitch of a pixel, covering half a subpixel B, a subpixels R, a subpixels G, a subpixels R, and half a subpixel B. The length (in the x-direction) is twenty times the width. Four side boundaries of the model are set to have completely specular reflective properties so that the simulation model can be equivalent to an identical model extending transversely and longitudinally. Moreover, the simulation model takes both Fresnel loss and material absorption into account. The following paragraphs detail parameters of the elements in the two models, simulation results, and discussion.

3.1 Simulation for Light Mixing-and-Collimating Element

In the model, the light mixing-and-collimating element made of PMMA (Poly Methyl Meth Acrylate) has the length (x-direction) of 470 mm, the width of 3.3 mm and thickness of 0.3 mm for the inlet, the width of 40 mm and thickness of 3.2 mm for the outlet. The thickness gradually increases to 3.2 mm from 0.3 mm within the front length of 28 mm; then the width gradually increases to 40 mm from 3.3 mm within the remaining length of 442 mm. The bottom surface has longitudinally extending micro V-grooves with a pitch of 0.05 mm and an apex angle of 140°. The light mixing-and-collimating element curves at a radius of 4000 mm; the emitting area of the LED contacts the inlet. Fig. 7 shows the simulation results about the illumination on the outlet and intensity of the light emerging from the outlet. Fig. 7(a) indicates the illuminance on the outlet along the central transverse line is uniform; the ratio of the minimum of the curve to the maximum is 0.91, but the bottom area has lower illuminance because of the curved body. Fig. 7(b) indicates the FWHM (full width at half maximum) of the both angular distribution reduces to 7° (measured in PMMA) in the transverse (horizontal) and vertical directions. Again, the curved body makes the angular distribution in the vertical broaden. However, its half-angle is below 6° (equivalent to 9° measured in the air) and satisfies the requirement for the following color separation. Moreover, our previous work has verified multiple elements arranged side by side can form an equivalently monolithic linear source that is uniform and collimated [16].

3.2 Simulation for Polarization-Converting Element

The polarization-converting element made of PMMA is attached to the outlets of the two precedent light mixing-and-collimating elements arranged side by side, and its dimensions are as follows:

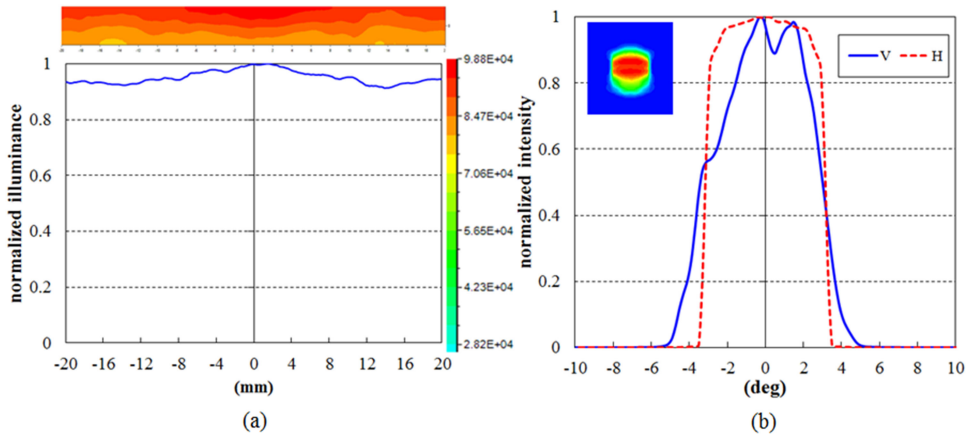

Fig. 7. Simulation results about light mixing-and-collimating element: (a) normalized illuminance on its outlet; (b) normalized intensity of the light emerging from its outlet.

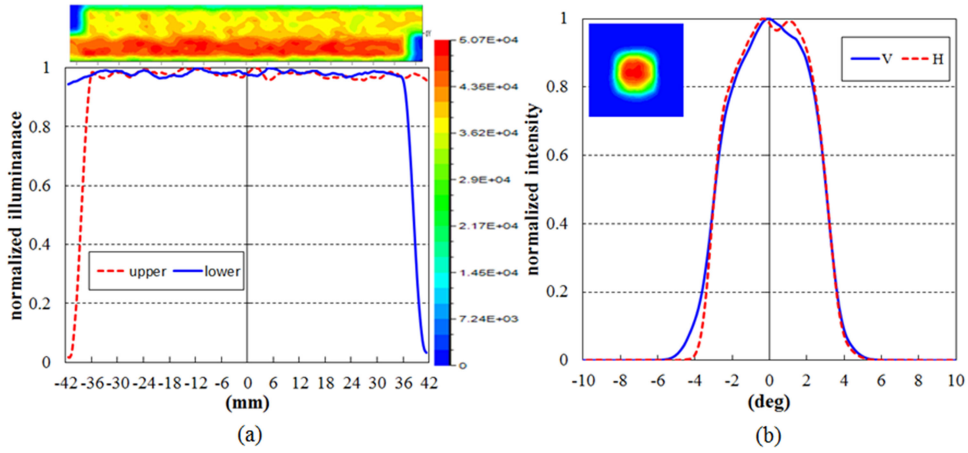

Fig. 8. Simulation results about polarization-converting element: (a) normalized illuminance on its outlet; (b) normalized intensity of the light emerging from its outlet.

the length of 9.7 mm, the width of 80 mm; the thickness of its inlet is 3.2 mm; the thickness of its outlet is 6.5 mm. Here the absorption of the reflective polarizing film is assumed 3% the same as the DBEF [12]. Fig. 8 shows the simulation results about the illumination on the outlet and intensity of the light emerging from the outlet. Fig. 8(a) indicates the illuminance on the outlet is uniform in the transverse direction, and the seam between the outlets of the two precedent light mixing-and-collimating elements does not appear. However, the value on the lower portion is higher than the upper portion because part of the light leaks out during its sequential reflection on the sloped facets before the light emerges from the upper portion. Fig. 8(b) indicates the both angular distribution is almost the same in the transverse (horizontal) and vertical directions, with an angular FWHM of 7° and a half-angle below 5.5° (measured in PMMA). Moreover, the DOP (Degree of Polarization) of the light exiting the polarization-converting element is 95%. The DOP is defined as follows:

$$DOP = \frac{flux_s - flux_P}{flux_s + flux_P} \times 100\% \tag{2}$$

where $flux_{\mathrm{S}}$ and $flux_{\mathrm{P}}$ are the luminous flux of s-wave and p-wave, respectively.

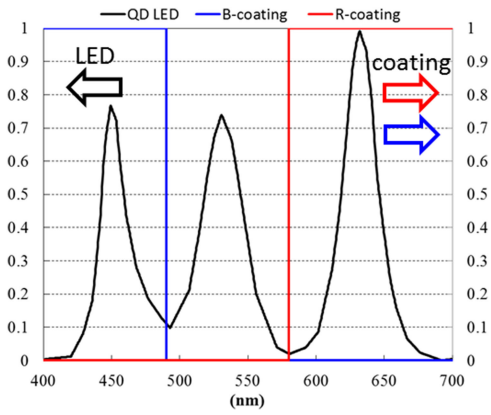

Fig. 9. Spectrum characteristics of light sources and the corresponding dichroic coating layers.

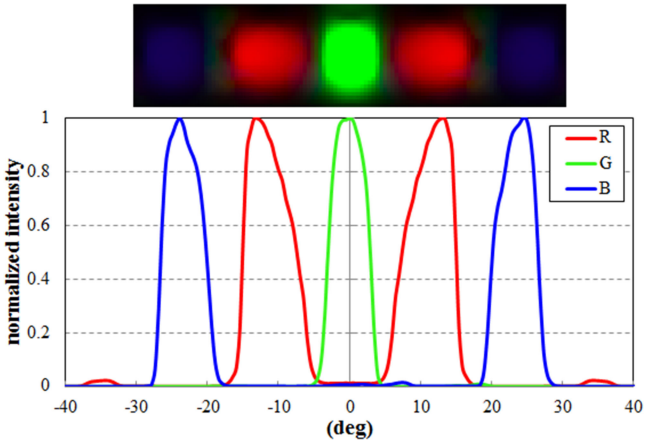

Fig. 10. Normalized intensity of the light emerging from the outlet of color-separating element.

3.3 Simulation for Color-Separating Element

The color-separating element made of PMMA connects with the outlet of the polarization-converting element, and its dimensions in *y*, *x*, and *z* directions are 80 mm $\times$ 21.5 mm $\times$ 16.5 mm. The angle-modulating component made of PMMA is in the middle layer of the element and sandwiched by two layers of optical adhesion with refractive index of 1.35. It has micro prisms of a 0.04-mm pitch thereon. The apex angles of the prisms in the portions illuminated by the beams B, R are 23° and 32°, respectively. Moreover, it has the lenticular lens arrays of a 0.65-mm pitch thereunder. The curvature radii in the portions illuminated by the beams B, R, and G are 5.7 mm, 2.4 mm and 1.2 mm, respectively. To enhance the color gamut, we modulated the reflective spectra of the dichroic coating layers in the element according to the spectrum of the light source. In this study, we assumed the white light source is an LED with color enhancement by quantum-dot technology (simply called 'QD WLED' hereafter) providing the same spectrum in a SONY LCD TV (model: KDL-55W900A). Fig. 9 shows the spectra of the LED and the reflective spectrum of the corresponding dichroic coating layers. Fig. 10 shows the simulation results about the intensity of the light emerging from the outlet of the color-separating element (measured in PMMA). In Fig. 10, one green beam is in the center of the angular space; two blue beams are at the outmost; the red beams are between the green and blue beams; they distribute in angular symmetry in the *xz*-plane. Although a little crosstalk exists between the color beams, it is acceptable because the black matrix on the LC panel can absorb the portion of the mixed color light.

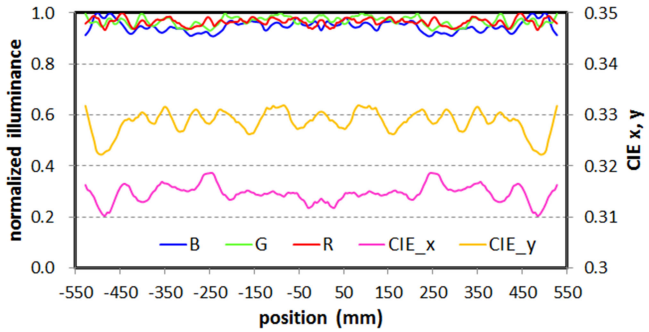

Fig. 11. Distribution of the illuminance and CIE xy of RBG beams on top surface of curved LGP.

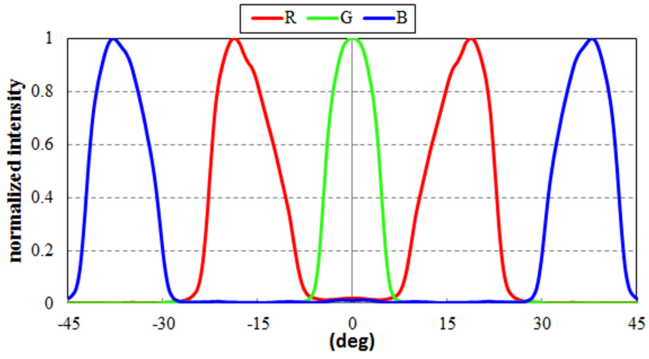

Fig. 12. Normalized intensity of the color beams emerging from top surface of curved LGP.

3.4 Curved LGP With Micro V-grooves

The curved LGP made of PMMA connects with the outlet of the color-separating element. Its dimensions in x, y, and z directions are 1100X80X6.5 (unit in mm); radius of curvature are 4000 mm. The LGP has micro isosceles V-grooves transversely extending on its bottom, whose pitch and apex angle are fixed to 0.025 mm and 93.6°, respectively. The intervals between the V-grooves vary to obtain good uniformity of illuminance on LGP top surface. To avoid dark areas (bandings) appear on the front surface of the light guide resulting in great luminance-non-uniformity, we adopted an equal-thickness LGP with light fed from its both ends in this study. Such design can greatly improve the difference in the density of V-grooves along the LGP, although its optical efficiency would be lower. In the model, the density of the V-grooves ranges from 0.33 to 0.8, and therefore the banding does not appear. Fig. 11 shows the simulation results about the distribution of the illuminance and values of CIE xy of the color beams emerging from the top surface of the curved LGP. The illuminance distribution of the red, green, and blue light is similar and uniform; color variation in CIE x and y of the mixed emerging light along the LGP is both below 0.01, which means it performs good uniformity of illuminance and color in the spatial space. The definition of the uniformity of illuminance is the percentage ratio of the minimum illuminance to the maximum; the illuminance uniformity of the R, G, and B is 93.3%, 93.1%, and 91.3%, respectively. Fig. 12 shows the simulation results about the intensity of the light emerging from the LGP. The five color beams B, R, G, R, and B emerge from the top surface of the curved LGP at different angles −36.3°, −18.1°, 0°, 18.1°, and 36.3° (measured in the air) with the z-axis in the transverse and have a little cross-talk between them. In addition, the color beams are wider in the x-direction as compared with the beams exiting the color-separating element because the curved LGP diffuses the beams in the x-direction.

TABLE 1
Parameters of the Integrated LC Panel in the Simulation

item	$\theta_1(=\theta_5)$	$\theta_2(=\theta_8)$	$\theta_3(=\theta_7)$	$\theta_4(=\theta_6)$	w_1	w_2	w_3
value	74°	85°	83°	84°	200 μm	90 μm	90 μm
item	w_r	w_g	w_b	w_{m1}	$w_{m2}(=w_{m3})$	w_{m4}	α
value	65 μm	60 μm	75 μm	82.5 μm	35 μm	82.5 μm	130°
item	l_p	h_p	h_t	h_λ	t_{s2}	t_{s1}	t_{LC}
value	500 μm	14.5 μm	250 μm	120 μm	200 μm	200 μm	400 μm

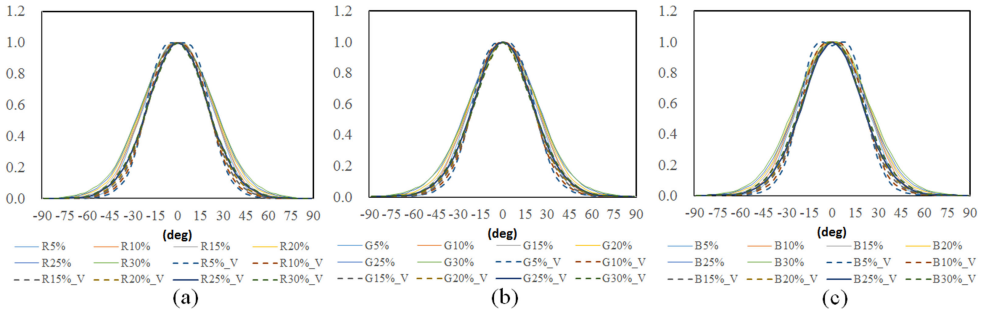

Fig. 13. Effect of the volume rate of scattering particles on angular distribution of the color beams emerging from integrated LC panel: (a) R; (b) G; (c) B.

3.5 Performance of Backlight Operating With Integrated Color-Filter-Free LC Panel

Table 1 lists the related parameters of the integrated LC panel described in Fig. 5. For simplicity, we set the refractive indices of the materials in the integrated LC panel model the same as PMMA. The pitch of one pixel is 500 μm; the aperture ratio is 0.53. Because the B color beams are incident at larger angles with *z*-axis than the G and R color beams, the focus condition of the B color beams is the worst. To improve the focus condition of the B color beams, we designed the lenticular lens with a free-form cross-sectional profile. Further, we also optimized the parameters of the light-reforming layer on the front surface of the LC panel to make the five color beams emerge out in the normal with the similar angular distribution, and thus ensured good color uniformity of the emerging light in the angular space. Because the B color beams have a larger angle with *z*-axis than the beams G and R, the parameters of the trapezoid corresponding to the blue subpixel, θ_1 and the ratio of w_b to w_1, must be smaller as compared with those corresponding to the red and green subpixels.

Fig. 13 shows the simulation results about the effect of the volume rate of scattering particles on the angular distribution of the color beams (R, G, and B) emerging from the integrated LC panel. The angular distribution of the color beams is very similar and spreads as the volume rate of scattering particles added in the top substrate. The particles are made of silica, and their average radius is 5 μm.

Next, we simulated the color distribution of the combined color beams (resultant light) emerging from the integrated LC panel in the angular space for various volume rates of scattering particles added in the top substrate. The simulation results indicate that the color variation in the angular space decreases with the volume rate of scattering particles. However, the higher volume rate of the scattering particles reduces the amount of the emerging light. Therefore, the volume rate at 20% is the optimal for the balance between the angular color uniformity and optical efficiency. With considering the optical efficiency of R, G, and B color beams in the system is different (especially in the DOP), we modulated the power spectra of the light source to make the resultant light reach white point in the simulation in this section. Fig. 14 shows the simulation result about the angular color distribution of the resultant light. If we limit the variation of the color coordinate x (CIE1931) below 0.01, the angular widths in the horizontal and vertical axis are 140° and 115°, respectively. Similarly, if we limit the variation of the color coordinate y (CIE1931) below 0.01, the angular widths

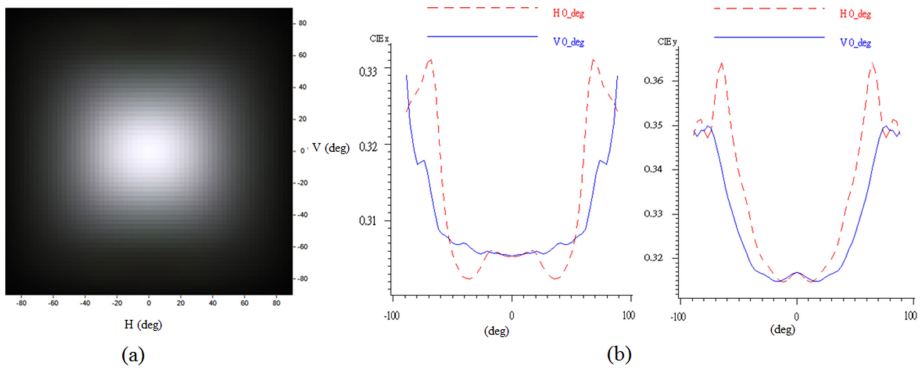

Fig. 14. Color intensity of the resultant light: (a) 2D intensity chart; (b) CIE xy of color intensity.

TABLE 2
Coordinates of RGB Subpixels for CIE 1931

	Color gamut of NTSC			LCD using QD WLED		
	R	G	B	R	G	B
x	0.67	0.21	0.14	0.646	0.212	0.156
y	0.33	0.71	0.08	0.294	0.673	0.036
area	0.1582			0.1488		

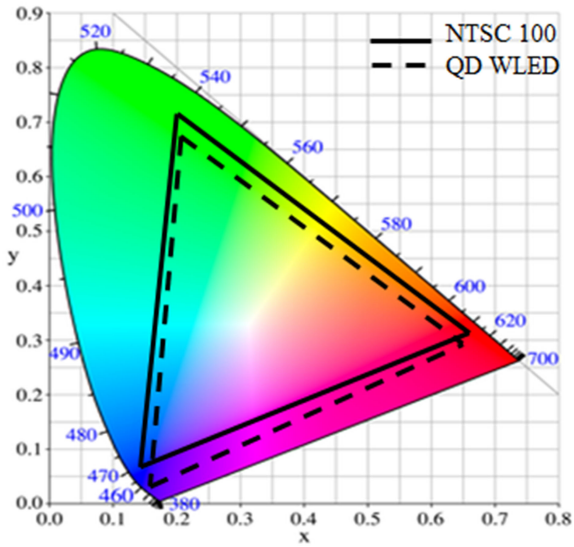

Fig. 15. Color gamut of the proposed LCD system.

in the horizontal and vertical directions are 100° and 75°, respectively. It means the proposed system provide good color uniformity within the angular widths of 100° and 75° in the horizontal and vertical directions, respectively.

After confirming the color uniformity in the angular space, we simulated the color coordinates for R, G, and B subpixels separately turned on alone to evaluate the color gamut of the proposed display system. Table 2 lists the color coordinates of the red, green, and blue colors in the optimal condition, and Fig. 15 plots the triangle of the color gamut displayed by the system. The triangle drawn by solid black lines is the CIE 1931 color gamut defined by the National Television System

TABLE 3
Optical Efficiency of Each Component in the Proposed LCD System

	Light mixing& collimating element	Polarization-converting element	Color-separating element	Curved LGP	Integrated LC panel	Entire system
efficiency	82.8%	93.74%	89.69%	77.27%	62.75%	33.75%

Committee (NTSC), while the triangle drawn using dashed black lines is the color gamut of the proposed display system. The area of the color gamut of the system is 94.1% of that defined by NTSC mainly because of lower saturation in green color. The crosstalk between the color beams leads to lower saturation in colors.

3.6 Efficiency Analysis

We analyze the optical efficiency of the components of the entire system from the simulation results in this section. The simulation considered the Fresnel loss and absorption of the material bulk. In addition, we assumed the light completely passed through the absorptive polarizer attached on the LC panel when its polarizing direction was the same as the transmission axis of the polarizer. The DOP of the color light emerging from the LGP affects the optical efficiency greatly. If there is no coating layer covering the micro V-grooves on the LGP bottom, the light hitting the V-grooves is reflected by TIR. However, TIR caused a different phase shift between the p-wave and s-wave, which causes the DOP of the light emerging from the LGP to depend on the angle between the *x*-axis and the direction of light propagating in the LGP; thereby the DOP of the green light is the highest and that of the blue light is the lowest. The DOP of the R, G, and B beams emerging from the LGP are 85%, 99%, 58%, respectively. Coating a 5-μm silver layer on the LGP bottom (including V-grooves) can resolve the issue; the DOP of the R, G, and B beams emerging from the LGP are 99%, 99%, 91%, respectively. Although the silver layer absorb 2.5% more light, the resultant polarized light emerging from the LGP increases 14.3%. Table 3 lists the efficiency of each component under the optimal condition. The optical efficiency of the entire system is 33.75% with only considering the portion of polarized light passing through the absorptive polarizer in the LC panel. The optical efficiency of the integrated LC panel is the lowest 62.75% because of low aperture ratio, absorption of the polarizer, and volume scattering in the top substrate. The curved LGP has the second lowest efficiency because we pursue good uniformity of illuminance instead of high efficiency.

To compare the optical efficiency of the proposed LCD system with that of the traditional LCD, we simulated the white light from a traditional backlight transmitted into an LCD with a color filter thereon. We assumed the light source of the traditional backlight was the QD WLED and the color filter had the transmissive spectrum shown as Fig. 16 [37]. The aperture ratio of the black matrix in the traditional LCD system was set 70%. The expression of total optical efficiency of the traditional LCD is as below:

$$\eta_{\text{total}} = \eta_{\text{backlight}} \times T_{LC} \times \frac{\int (P_R(\lambda) + P_G(\lambda) + P_B(\lambda)) \times T_{color}(\lambda) d\lambda}{\int (P_R(\lambda) + P_G(\lambda) + P_B(\lambda))\,(\lambda) d\lambda}. \tag{3}$$

The parameters P_{R}, P_{G}, and P_{B} denote the power of the red, green, and blue light, respectively; $T_{\mathrm{color}}(\lambda)$ is the transmissive spectrum of the color filter, T_{LC} is the transmission of the LC panel, and $\eta_{\mathrm{backlight}}$ is the optical efficiency of the backlight. In the simulation, we assumed absorption in the LC panel entirely from the black matrix and polarizer, so T_{LC} is 0.35 for an unpolarized backlight when the black matrix has a 70% aperture ratio. The optical efficiency of a slim-type backlight is generally 80% [38]. Consequently, the calculated total optical efficiency of the traditional LCD is only 8.44%, which is about one-fourth of the proposed LCD system. In addition, the color gamut dramatically drops to 84.1% because of the transmissive spectrum of the color filter is not optimized for the spectrum of the QD WLED.

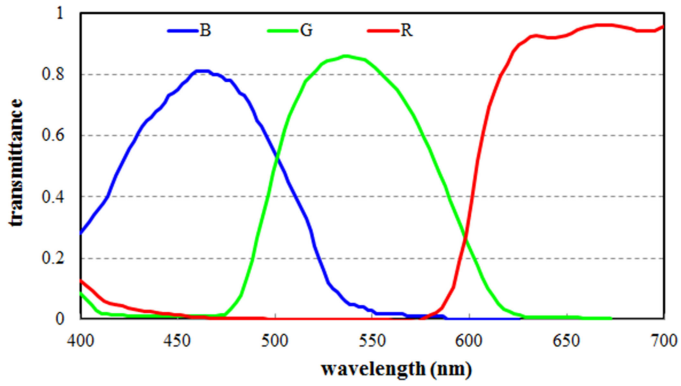

Fig. 16. Transmissive spectrum of the color filter.

4. Conclusion

In this study, we proposed an LCD system combining a polarized color-separating backlight and an integrated color-filter-free LC panel for performing high optical efficiency and wide color gamut. The optical model of the LCD system was established and the simulation was implemented for verifying feasibility of the idea. In the simulation model, the backlight has a length of 1120 mm and a width of 80 mm, including a 1100X80X6.5 (unit in mm) LGP with a curvature radius of 4000 mm. The thickness of the most portion of the backlight is below 10 mm except for the 28 mm-wide edge portion with a maximal thickness of 16.5 mm; the minimal thickness is only 6.5 mm. Moreover, the thickness of the entire system should add the 1.2 mm thickness of the integrated LC panel. The model can extend in the transverse direction for large-sized application while keeping the same performance. Because the thickness of the proposed backlight mainly depends on that of the emitting area of an LED, a miniaturized LED such as mini LED can further reduce the entire thickness. This study demonstrated that the proposed LCD system reached three major achievements:

1) It performs the high optical efficiency of 33.75% that is about four times the traditional LCD, and displays color gamut of 94.1% NTSC (CIE 1931).
2) It demonstrates the illuminance uniformity exceeding 0.9; provides good color uniformity in both spatial space and angular space of the viewing cone with horizontal and vertical angular widths of 100° and 75°, respectively.
3) For the ratio of the width to the height in the screen 16:9, it can apply to a 55-inch curved LCD, and extend the maximum diagonal size up to 88 inches for a flat-type one with the light fed from the two long edges while keeping slim volume with a minimal thickness of 6.5 mm.

Therefore, this study proved that the proposed LCD system is a competitive solution for the LCD to greatly improve the entire optical efficiency and provide wide color gamut, which is important for a new-fashioned large-sized curved LCD to become an environmentally friendly and high-quality product.

References

[1] H. W. Chen, J. H. Lee, B. Y. Lin, S. Chen, and S. T. Wu, "Liquid crystal display and organic light-emitting diode display: Present status and future perspectives," *Light: Sci. Appl.*, vol. 7, 2018, Art. no. 17168.
[2] 3M, "Display with reflective polarizer and randomizing cavity," U.S. Patent 6025897, Feb. 15, 2000.
[3] Y. Li, T. X. Wu, and S. T. Wu, "Design optimization of reflective polarizers for LCD backlight recycling," *J. Display Technol.*, vol. 5, no. 8, pp. 335–340, 2009.
[4] K. W. Chien, H. P. D. Shieh, and H. Cornelissen, "Polarized backlight based on selective total internal reflection at microgrooves," *Appl. Opt.*, vol. 43, pp. 4672–4676, 2004.
[5] S. Hwang, Y. T. Kim, S. Nam, and S. D. Lee, "Polarized light out-coupling in backlight by collimating the beam into light guide plate," *J. Soc. Inf. Display*, vol. 8, no. 1, pp. 18–21, 2007.

[6] H. J. Cornelissen, H. J. B. Jagt, D. J. Broer, and C.W. M. Bastiaansen, "Efficient and cost-effective polarized-light backlights for LCDs," *Proc. SPIE*, vol. 7058, 2008, Art. no. 70580X.
[7] H. Jagt, H. J. Cornelissen, D. J. Broer, and C. Bastiaansen, "Linearly polarized light-emitting backlight," *J. Soc. Inf. Display*, vol. 10, no. 1, pp. 107–112, 2012.
[8] K.W. Chien and H. P. D. Shieh, "Design and fabrication of an integrated polarized light guide for liquid-crystal-display illumination," *Appl. Opt.*, vol. 43, pp. 1830–1834, 2004.
[9] X. Yang, Y. Yan, and G. Jin, "Polarized light-guide plate for liquid crystal display," *Opt. Exp.*, vol. 13, no. 21, pp. 8349–8356, 2005.
[10] C. H. Chen, P. C. Chen, and C. C. Chen, "High extinction ratio polarized light guide with layered cross stacking nanostructure," *Microelectron. Eng.*, vol. 86, pp. 1107–1110, 2009.
[11] S. H. Kim, J. D. Park, and K. D. Lee, "Fabrication of a nano-wire grid polarizer for brightness enhancement in liquid crystal display," *Nanotechnology*, vol. 17, pp. 4436–4438, 2006.
[12] J. S. Seo, T. E. Yeom, and J. H. Ko, "Experimental and simulation study of the optical performances of a wide grid polarizer as a luminance enhancement film for LCD backlight applications," *J. Opt. Soc. Korea*, vol. 16, pp. 151–156, 2012.
[13] P. H. Yao, C. J. Chung, C. L. Wu, and C. H. Chen, "Polarized backlight with constrained angular divergence for enhancement of light extraction efficiency from wire grid polarizer," *Opt. Exp.*, vol. 20, pp. 4819–4829, 2012.
[14] Z. Luo, Y. Cheng, and S. Wu, "Polarization-preserving light guide plate for a linearly polarized backlight," *J. Display Technol.*, vol. 10, no. 3, pp. 208–214, 2014.
[15] T. Kurashima, K. Sakuma, T. Arai, A. Tagaya, and Y. Koike, "A polarized laser backlight using a zero–zero-birefringence polymer for liquid crystal displays," *Opt. Rev.*, vol. 19, no. 6, pp. 415–418, 2012.
[16] T. C. Teng and L. W. Tseng, "Slim planar apparatus for converting LED light into collimated polarized light uniformly emitted from its top surface," *Opt. Exp.*, vol. 22, no. S6, pp. A1477–A1490, 2014.
[17] C. H. Chen, F. C. Lin, Y. T. Hsu, Y. P. Huang, and H.-P. D. Shieh, "A field sequential color LCD based on color field arrangement for color breakup and flicker reduction," *J. Display Technol.*, vol. 5, pp. 34–39, 2009.
[18] H. Dammann, "Color separation gratings," *Appl. Opt.*, vol. 17, no. 15, pp. 2273–2279, 1978.
[19] H. H. Lin and M. H. Lu, "Design of hybrid grating for color filter application in liquid crystal display," *Jpn. J. Appl. Phys.*, vol. 46, no. 8B, pp. 5414–5418, 2007.
[20] M. Xu, H. P. Urbach, and D. K. de Boer, "Simulations of birefringent gratings as polarizing color separator in backlight for flat-panel displays," *Opt. Exp.*, vol. 15, no. 9, pp. 5789–5800, 2007.
[21] R. Caputo, L. D. Sio, M. J. J. Jak, E. J. Hornix, D. K. G. De Boer, and H. J. Cornelissen, "Short period holographic structures for backlight display applications," *Opt. Exp.*, vol. 15, no. 17, pp. 10540–10552, 2007.
[22] M. J. J. Jak, R. Caputo, E. J. Hornix, L. de Sio, D. K. G. de Boer, and H. J. Cornelissen, "Color-separating backlight for improved LCD efficiency," *J. Soc. Inf. Display*, vol. 16, no. 8, pp. 803–810, 2008.
[23] H. H. Lin, C. H. Lee, and M. H. Lu, "Dye-less color filter fabricated by roll-to-roll imprinting for liquid crystal display applications," *Opt. Exp.*, vol. 17, no. 15, pp. 12397–12406, 2009.
[24] C. W. Liu, C. H. Lee, C. J. Ting, T. H. Lin, and S. C. Lin, "Roll-to-roll process-based sub-wavelength grating for a color-separation backlight," *J. Display Technol.*, vol. 9, no. 7, pp. 561–564, 2013.
[25] C. G. Son, J. S. Gwag, J. H. Lee, and J. H. Kwon, "Analysis of a color-matching backlight system using a blazed grating and a lenticular lens array," *Appl. Opt.*, vol. 51, no. 36, pp. 8615–8620, 2012.
[26] P. C. Chen, H. H. Lin, C. H. Chen, C. H. Lee, and M. H. Lu, "Color separation system with angularly positioned light source module for pixelized backlighting," *Opt. Exp.*, vol. 18, no. 2, pp. 645–655, 2010.
[27] A. Travis, T. Large, N. Emerton, and S. Bathiche, "Collimated light from a waveguide for a display backlight," *Opt. Exp.*, vol. 17, no. 22, pp. 19714–19719, 2009.
[28] T. C. Teng and L. W. Tseng, "Planar apparatus for uniformly emitting light with angular color-separation," *Opt. Exp.*, vol. 23, no. 11, pp. A553–A568, 2015.
[29] H. J. Jeon, G. Park, and J. H. Kwon, "Color-matching liquid crystal display using a lenticular lens array," *J. Opt. Soc. Korea*, vol. 18, no. 4, pp. 345–349, 2014.
[30] Z. Luo, G. Zhang, R. Zhu, Y. Gao, and S. T. Wu, "Polarizing grating color filters with large acceptance angle and high transmittance," *Appl. Opt.*, vol. 55, no. 1, pp. 70–76, 2016.
[31] Y. Kanamori, M. Shimono, and K. Hane, "Fabrication of transmission color filters using silicon subwavelength gratings on quartz substrates," *IEEE Photon. Technol. Lett.*, vol. 18, no. 20, pp. 2126–2128, Oct. 2006.
[32] Y. Ye, Y. Zhou, and L. S. Chen, "Polarizing color filter based on a subwavelength metal-dielectric grating," *Appl. Opt.*, vol. 50, pp. 1356–1363, 2011.
[33] R. Girard-Desprolet, S. Boutami, S. Lhostis, and G. Vitrant, "Angular and polarization properties of cross-holes nanostructured metallic filters," *Opt. Exp.*, vol. 21, pp. 29412–29424, 2013.
[34] J. Lee, K. Lee, S. Seo, and L. Guo, "Decorative power generating panels creating angle insensitive transmissive colors," *Sci. Rep.*, vol. 4, 2014, Art. no. 4192.
[35] M. Y. Yu, B. W. Lee, J. H. Lee, and J. H. Ko, "Correlation between the performance of the optical reflective polarizer and the structure of the LCD backlight," *J. Opt. Soc. Korea*, vol. 13, no. 2, pp. 256–260, 2009.
[36] B. W. Lee, M. Y. Yu, and J. H. Ko, "Dependence of the gain factor of the reflective polarizer on the configuration of optical sheets," *J. Soc. Inf. Display*, vol. 10, no. 1, pp. 28–32, 2009.
[37] 2019. [Online]. Avaialble: https://www.synopsys.com/optical-solutions/lighttools/feature-details.html
[38] D. Grabovičkić, P. Benítez, J. C. Miñano, and J. Chaves, "LED backlight designs with the flow-line method," *Opt. Exp.*, vol. 20, no. S1, pp. A62–A68, 2012.